Relaxation Phenomena of Stereoregular Poly(methyl methacrylate) Monolayers at the Air/Water Interface

Yuh-Lang Lee,[1] Wen-Ping Hsu[2]

[1]Department of Chemical Engineering, National Cheng Kung University, Tainan, Taiwan 70101, Republic of China
[2]Department of Chemical Engineering, National United University, Miao-Li, Taiwan 36003, Republic of China

ABSTRACT: Relaxation behaviors of isotactic, atactic, and syndiotactic poly(methyl methacrylate) (PMMA) monolayers at the air/water interface were investigated at three different temperatures. The monolayer characteristics of the three stereoisomers were studied in terms of surface pressure–area per molecule (π-A) isotherm, area relaxation, and pressure relaxation. The results show that pressures at inflection points of π-A isotherms of PMMA decrease with an increase in temperature. The collapse pressure also decreases as the temperature is elevated. It was shown likely for the first time that the relaxation process of PMMA stereoisomers could be described by a model considering the nucleation and growth mechanisms. The simulation parameters of area relaxation of the three stereoisomers at 30 mN/m are very similar, indicating similar mechanisms. © 2007 Wiley Periodicals, Inc. J Appl Polym Sci 107: 37–44, 2008

Key words: relaxation; stereoregular; PMMA; monolayer

INTRODUCTION

Monolayer films of polymers have been the subject of extensive research during the past decades,[1,2] but the research efforts have increased rapidly because of possible applications in nonlinear optical devices and other fields such as biosensors and microlithography.

Crisp[1,2] was the first to systematically investigate monolayer properties of polymers, especially of polyacrylates and polymethacrylates. He showed that poly(methyl methacrylate) (PMMA) forms patchy structures, composed of condensed islands of PMMA at low surface coverages. He also proposed conformations for the ester groups in these materials at the air–water interface, based on measurements of the dipole moments. Since then a lot of articles have been published about PMMA monolayers at the air–water surface, such as its monolayer miscibility with low molecular weight substances and other polymers, the stability and hysteresis that may occur,[3–6] and so on.

With all this work on PMMA, the matter of tacticity of the polymers had seldom been addressed. Beredjick et al.[7] published isotherms of isotactic, atactic, and syndiotactic PMMA in 1960: the pressure–area (π-A) isotherms of the isotatic polymer showed to be quite different from those of atactic and syndiotactic samples. Sutherland and Miller[8] also reported isotherms for isotactic and atactic PMMA and found their results in agreement with the observations of Beredjick et al.[7]

Around 1990, Brinkhuis and Schouten reported extensive studies of thin film behavior of PMMA of varying tacticity,[9] crystallization of isotactic PMMA in mixed monolayers,[10] and stereocomplexation of isotactic and syndiotactic PMMA.[11]

In a previous study of our report,[12] behaviors of isotactic, atactic, and syndiotactic PMMA monolayers at the air/water surface were investigated at 25 and 40°C. The monolayer characteristics of the three stereoisomers were studied and compared in terms of surface pressure–area per molecule (π-A) isotherm, hysteresis and relaxation phenomena, and the phase images observed from Brewster angle microscopy (BAM). The area relaxation behaviors of PMMA stereoisomers were only studied qualitatively.

In this article, in the continuation of previous study, we investigated the relaxation phenomenon at three temperatures (one additional temperature at 10°C) quantitatively. Not only area relaxation experiments were performed, but also measurements of pressure relaxation were carried out. To the best of our knowledge, there is no systematic and detailed report on the area and pressure relaxation of stereoregular PMMA monolayers at the air–water interface at three temperatures. Therefore, in this investigation, monolayer films of stereoregular PMMA were

studied in terms of surface pressure–area per molecule (π-A) isotherms, area, and pressure relaxations. Area relaxation was performed by maintaining the surface pressure at constant and observing area change as a function of time. Pressure relaxation experiments were studied by keeping the surface area unchanged at a predetermined initial pressure. The results were simulated by an Avrami analysis.[13–15] The experimental observations indicated that the mechanisms for area and pressure relaxation phenomena were similar.

EXPERIMENTAL

Materials

Isotactic PMMA, atactic PMMA, and syndiotactic PMMA (designated as iPMMA, aPMMA, and sPMMA, respectively, in this study) were purchased from Polysciences, Warrington, PA. According to the supplier information, the molecular weights (M_w) of iPMMA, aPMMA, and sPMMA are the same about 100,000 g/mol.

The polydispersities (M_w/M_n) of the three PMMAs were not measured and therefore they are not reported here. However, the molecular weight distribution effect is believed to be minimal in the current study when compared with the effect of tacticity. We did not characterize the tacticity of PMMA by NMR. Therefore, a simple estimation of the fractions of meso (m) and racemic (r) diads was resorted. The meso diad fractions of PMMA were computed previously.[16] The m and r fractions of iPMMA, aPMMA, and sPMMA are 68.7% and 31.3%, 33.8% and 66.2%, 9.3% and 90.7%, respectively. The error of estimation is 5–8%. The glass transition temperatures (T_gs) of bulk iPMMA, aPMMA, and sPMMA were determined to be 75, 103, and 122°C, respectively, with a DuPont 2000 thermal analyzer at a heating rate of 20°C/min. The inflection point of the specific heat jump of the second thermal scan was taken as T_g. According to the study of Grohens et al.,[17] T_gs of stereoregular PMMAs depend on the film thickness. Therefore, the T_gs of the three PMMA stereoisomers are expected to be lower than those of bulk PMMA.

2-Butanone purchased from Kanto Chemical was used as the spreading solvent for the polymer films. Only highly pure water, which was purified by means of a Milli-Q plus water purification system, with a resistivity of 18.2 MΩ cm was used in all experiments.

Methods

A model minitrough was purchased from KSV Instruments, Finland. The Teflon trough was 320-mm long and 75-mm wide. Regulation of the trough temperature was controlled by circulating constant temperature water from an external circulator through the tubes attached to the aluminum-based plate of the trough. The trough was placed on an isolated vibration-free table and was enclosed in a glass chamber to avoid contaminants from the air. A computer with an interface unit obtained from KSV Instruments was used to control the Teflon barriers. One of the important characteristics of the trough system is that two barriers confining a monolayer at the interface are driven symmetrically during the compression of the monolayer. The surface pressure was measured by the Wilhelmy plate method. The resolution for surface measurement is 0.004 mN/m, and the inaccuracy of surface area regulation is less than 1%, according to the specifications of the instruments. A surface pressure–area per molecule (π-A) isotherm was obtained by a continuous compression of a monolayer at the interface by two barriers. Before each isotherm measurement, the trough and barriers were cleaned with an ethanol solution and then rinsed by purified water. The sand-blasted platinum plate used for surface pressure measurements was also rinsed with purified water and then flamed before use. In addition, all glassware was cleaned prior to use in the same manner as the trough and barrier.

For starting the experiment, the freshly cleaned trough was placed into position in the apparatus first, then it was filled with purified water as the subphase with temperatures controlled at (10 ± 1)°C, (25 ± 1)°C, and (40 ± 1)°C. The clean platinum plate was hanged in the appropriate position for surface pressure measurements. The surface pressure fluctuation was estimated to be less than 0.2 mN/m during the compression of the entire trough surface area range. Then, the two barriers were moved back to their initial positions, and a sample containing monolayer-forming materials was spread on the subphase by using a Hamilton microsyringe. At least 40 min was allowed for evaporation of the spreading solvent. After the solvent was evaporated, the monolayer was compressed continuously at a rate of 3.5 mm/min to obtain a single π-A isotherm. The π-A isotherms of our studied polymers are dependent on the compression rate therefore the results were performed at the same compression speed.

Relaxation curves of monolayer films were also obtained in the same way as π-A isotherms. The only difference is that when the desired surface pressure was obtained and set as constant. Again, the relaxation curves should have some dependence on the original compression rate. Therefore, the same compression speed was used for all the investigations. Then A/A_0 ratio was monitored as a function of time, where A_0 is the initial surface area occupied by monolayer and A is the surface area of monolayer

at time t. For pressure relaxation curves, area at the same initial pressure was set. Then π/π_0 ratio was recorded as a function of time, where π_0 is the initial surface pressure and π is the surface pressure of monolayer at time t.

RESULTS AND DISCUSSION

π-A isotherms

The π-A isotherms of monolayers for the three PMMA stereoisomers are shown in Figure 1(a–c) at 10, 25, and 40°C, respectively. The results could be presented by plotting the same PMMA stereoisomers at three temperatures. However, we resorted to estimating monolayer characteristics of stereoregular PMMA at three temperatures and the results are shown later in Table I. According to Figure 1, iPMMA exhibits the most expanded and compressible characteristics among the three stereoisomers, and sPMMA is the least one. Therefore, iPMMA experiences ''good solvent'' conditions and forms an expanded type monolayer, whereas sPMMA forms a condensed monolayer, a difference that was attributed to a much higher level of the lateral cohesive interactions between the segments of the syndiotactic polymer. At low surface pressure, the occupied area per repeat unit for the three stereoisomers increases in the order: sPMMA < aPMMA < iPMMA. However, at high surface pressure (>20 mN/m), an opposite order is obtained. These results are consistent with that reported by Beredjick et al.[7]

Monolayer characteristics of stereoregular PMMA at three temperatures were estimated and tabulated in Table I. The collapse pressure decreases as a result of temperature elevation. At the three studied temperatures, iPMMA has the highest collapse pressure among three stereoisomers. Because of the higher compressibility of iPMMA, distinct segments are exhibited along the isotherm. Our aPMMA sample is similar to iPMMA because of tacticity distribution also demonstrating distinct segments. Two inflection points were detected both in iPMMA and aPMMA monolayers. The transition observed at about 8–9 mN/m is characteristic for the isotherms of iPMMA in contrast to the syndiotactic samples, which has no such phenomenon at low surface pressures. The isotherm for sPMMA exhibits a steep curve indicating the formation of a condensed monolayer. A phase transition point in the middle divides the isotherm into two segments. The pressures at inflection or phase transition points for the three stereoisomers decrease mostly as the temperature is increased. The effect is more marked between 10 and 25°C than between 25 and 40°C. The limiting areas (as shown in Table I) also exhibit similar temperature dependence, i.e., decreasing with increasing
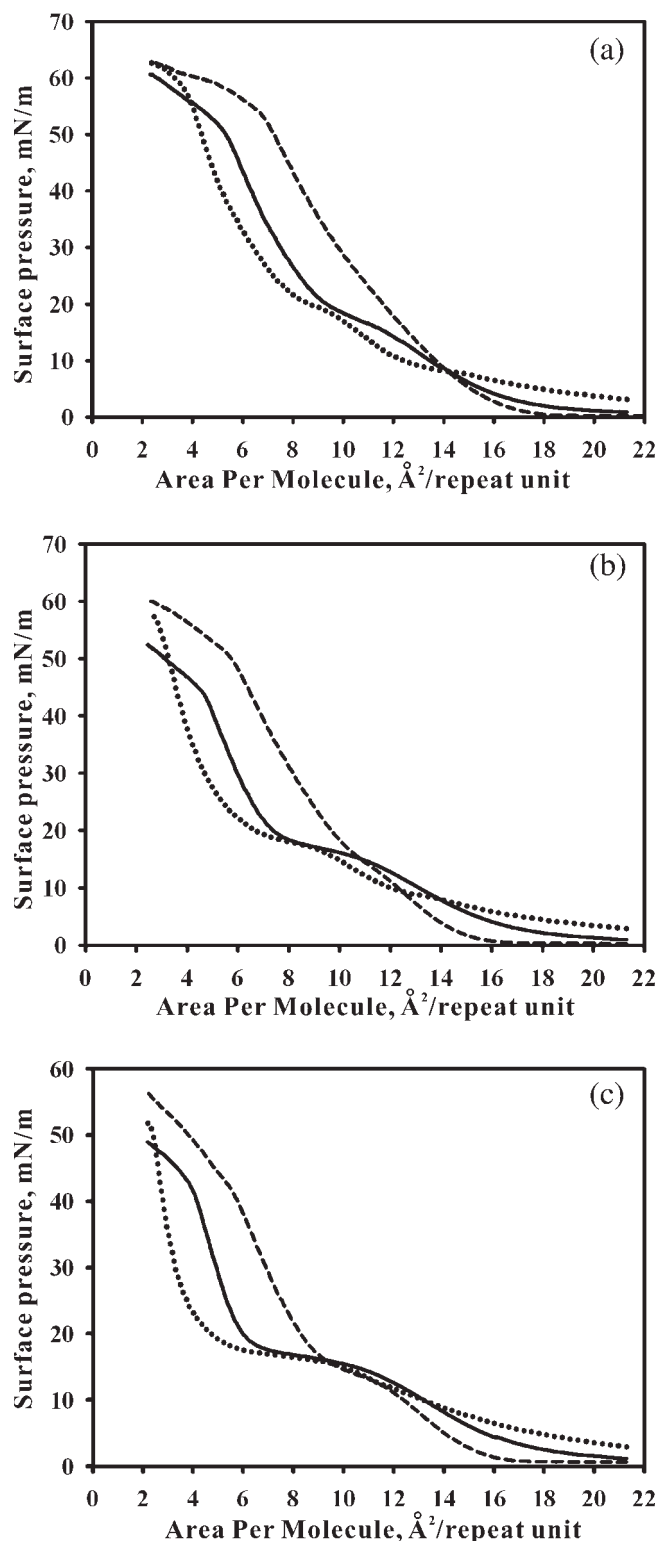

Figure 1 (a) π-A isotherms of stereoregular PMMA at 10°C (•••: iPMMA; ——: aPMMA; – – –: sPMMA0). (b) π-A isotherms of stereoregular PMMA at 25°C [symbols as in Fig. 1(a)]. (c) π-A isotherms of stereoregular PMMA at 40°C [symbols as in Fig. 1(a)].

temperature. sPMMA has the largest limiting area and iPMMA exhibits the smallest limiting area. It is interesting to observe that sPMMA exhibits two

TABLE I
Monolayer Characteristics of Stereoregular PMMA at Various Temperatures

		π Collapse (mN/m)	Inflection point (mN/m)		Limiting area (Å^2/ repeat unit)
10°C	aPMMA	51.0	9.4	16.4	10.3
	iPMMA	60.0	7.6	14.9	6.9
	sPMMA	54.5		15.5	12.8
25°C	aPMMA	43.0	7.5	16.4	8.5
	iPMMA	57.9	5.9	14.4	5.9
	sPMMA	51		14.9	11.3
40°C	aPMMA	41	6.5	16.7	7.1
	iPMMA	51	5.0	15.6	4.4
	sPMMA	42	8.4	15.3	10.3

inflection points similar to iPMMA (or aPMMA) at 40°C.

Area relaxation phenomenon

Area relaxation curves of three stereoisomers at a fixed surface pressure of 30 mN/m were given in Figure 2(a–c) in the order of 10, 25, and 40°C, respectively. At 10°C, the A/A_0 values after 90 min can be ranked as the following: aPMMA > sPMMA > iPMMA. The highest area loss of iPMMA may be attributed to its flexible side chain motion. However, the orders of the A/A_0 values at 25 and 40°C after 90 min are different and listed as follows: sPMMA > aPMMA > iPMMA (25°C) and sPMMA > aPMMA > iPMMA (40°C). At 25°C, aPMMA has a higher area loss (lower stability) than that of sPMMA. Such results can be explained by their values of T_gs (flexibility). At 40°C, it is interesting to observe that the area loss of aPMMA is approaching that of iPMMA. An attempt was made to interpret our relaxation results in more detail with respect to particle nucleation/growth models. Vollhardt and Retter[18–20] presented a series of studies describing the relaxation of stearic acid monolayers in the collapse region. They related the measurable loss of normalized area to the overall growth rate of 3D particles (clusters), considering different rate laws of the initial nucleation (instantaneous or progressive), the geometry of the growing clusters, and the overlap of the grown particles (clusters). Their theory led to a generalized equation for any nucleation model of the form exactly the same as the Avrami equation[13–15]

$$(A_0 - A)/(A_0 - A_\infty) = 1 - \exp(-k_x t^x) \qquad (1)$$

where A is the total surface area at time t, A_0 is the initial surface area, A_∞ is the area at $t \approx \infty$, and k_x is a constant specific for the applied geometry and nucleation model represented by the characteristic

exponent x. The characteristic exponent x varies from 1.5 to 4 in the Vollhardt's original derivation.

The simulated attempt (data taken from Fig. 2) by eq. (1) was demonstrated in Figure 3 as an example.
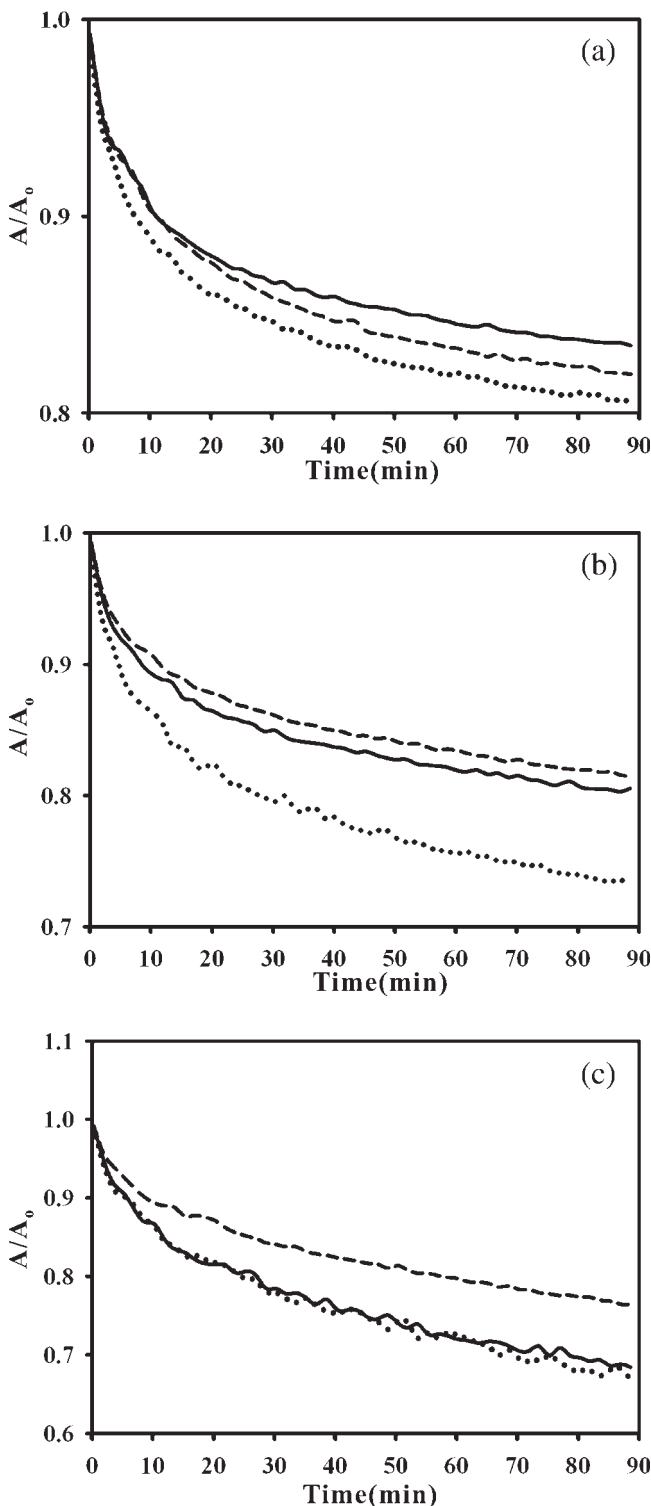

Figure 2 (a) Area relaxation curves at 30 mN/m (10°C) [symbols as in Fig. 1(a)]. (b) Area relaxation curves at 30 mN/m (25°C) [symbols as in Fig. 1(a)]. (c) Area relaxation curves at 30 mN/m (40°C) [symbols as in Fig. 1(a)].
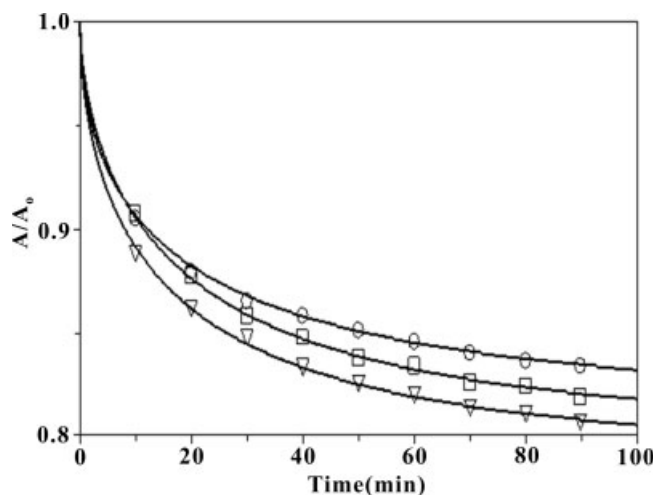
Figure 3 Simulation curves versus relaxation data ($\triangledown$: iPMMA; $\bigcirc$: aPMMA; $\square$: sPMMA).

The data points were shown at an interval of 10 min and the simulated results were represented by the solid lines. The estimated k_x and x values were listed in Table II. On the basis of correlation coefficient (R) and standard error (S), the agreement between simulation and experimental data is very good. The x values at 30 mN/m are between 0.5 and 0.6 for the three PMMA. The exact nucleation mechanism corresponding to these time exponents was not described by Vollhardt et al. or by other models in the literature. That is, the PMMA monolayers may relax in a more complicated mechanism than the model proposed for the relaxation of simple molecules.

The area losses of the monolayers estimated by A_{∞}/A indicates that the stability of the monolayers decrease as a result of temperature elevation, indicating the higher nucleation and growth rates of the aggregates at higher temperature and at $\pi = 30$ mN/m. This result is reasonable since a high mobility of PMMA molecules at high temperature is advantageous to the growth of clusters in the relaxation process. The three stereoisomers have similar A_{∞}/A values at low temperature (10°C). However, sPMMA seems to be the most stable one at elevated temperature (40°C), attributable to a more rigid characteristic resulting from its higher glass transition temperature (T_g) compared with the others. By means of two exponential equations, slight improvement of correlation and standard error can still be made. However, more variables will make physical explanations more complex. Therefore, the results are not included.

Area relaxation curves of three stereoisomers at a lower surface pressure of 10 mN/m were given in Figure 4(a–c) in the order of 10, 25, and 40°C, respectively. Comparing with the result obtained at $\pi = 30$ mN/m, the area losses of the PMMA mono-

layers after the relaxation reduce significantly at $\pi = 10$ mN/m. Especially, for aPMMA and sPMMA, the area losses are less than 3% and nearly independent of the temperature. Apparently, the nucleation and growth rates of the 3D aggregates are decreased due to the surface pressure decrease. The results were also simulated by eq. (1) except the aPMMA monolayer at 25°C. The aPMMA monolayer films at 25°C exhibit very stable structure and the area reduction is negligible. The computed k_x and x values were listed in Table III. On the basis of R and S values, the agreement is satisfactory. The x values at 10 mN/m are between 0.57 and 0.85, slightly larger than those at 30 mN/m. In general, the similar x values (0.5–0.6) at $\pi = 10$ mN/m to those obtained at $\pi = 30$ mN/m may imply the similar relaxation mechanism for the three stereoisomers at various temperatures. At $\pi = 10$ mN/m, the x values are still at the same range (0.5–0.6) for some systems, but higher values ranging between 0.7 and 0.8 are also observed, indicating possibly a shift of the relaxation mechanism.

Pressure relaxation phenomena

Pressure relaxation curves measured by fixing area at initial pressures of 30 and 10 mN/m were carried out at three temperatures (10°C, 25°C and 40°C) and the results at 40°C are shown in Figures 5 and 6 for representation. For the low initial pressure ($\pi = 10$ mN/m), sPMMA has a smaller pressure loss, compared with iPMMA, after 90 min relaxation. Besides, sPMMA seems to be the only one that can approach the equilibrium state within 90 min. However, the situation is different when the initial surface pressure is controlled at 30 mN/m. At this pressure, the iPMMA monolayer exhibits the smallest pressure loss and the sPMMA shows the highest one.

Theoretically, if the relaxation time is long enough, it is possible to reach the equilibrium surface pres-

TABLE II
Modeling Parameters of Area Relaxation of PMMA at 30 mN/m at 10, 25, and 40°C

		A_{∞}/A_0	k_x	x	R	S
10°C	aPMMA	0.8141	0.207	0.527	0.9982	0.0019
	iPMMA	0.7916	0.200	0.566	0.9988	0.0018
	sPMMA	0.8040	0.163	0.605	0.9994	0.0013
25°C	aPMMA	0.7587	0.182	0.495	0.9980	0.0024
	iPMMA	0.6915	0.173	0.538	0.9985	0.0029
	sPMMA	0.7667	0.161	0.505	0.9986	0.0019
40°C	aPMMA	0.4359	0.085	0.506	0.9969	0.0055
	iPMMA	0.5097	0.092	0.548	0.9968	0.0058
	sPMMA	0.6407	0.092	0.540	0.9985	0.0028

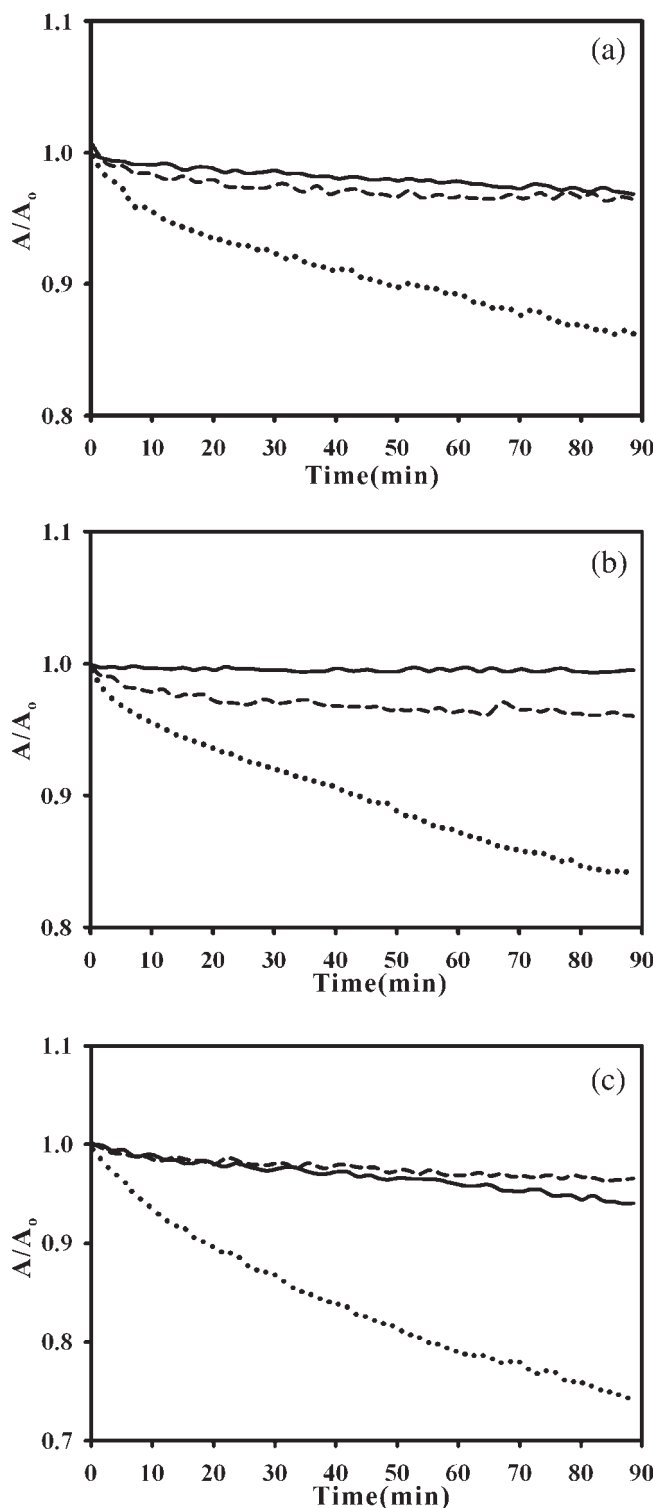R = correlation coefficient; S = standard error.

Figure 4 (a) Area relaxation curves at 10 mN/m (10°C) [symbols as in Fig. 1(a)]. (b) Area relaxation curves at 10 mN/m (25°C) [symbols as in Fig. 1(a)]. (c) Area relaxation curves at 10 mN/m (40°C) [symbols as in Fig. 1(a)].

TABLE III
Modeling Parameters of Area Relaxation of PMMA at 10 mN/m at 10, 25, and 40°C

		A_∞/A_0	k_x	x	R	S
10°C	aPMMA	0.8777	0.020	0.583	0.9858	0.0012
	iPMMA	0.4566	0.021	0.582	0.9967	0.0027
	sPMMA	0.9632	0.113	0.731	0.9786	0.0016
25°C	aPMMA	0.9942				
	iPMMA	0.6357	0.021	0.734	0.9964	0.0035
	sPMMA	0.9592	0.188	0.574	0.9688	0.0019
40°C	aPMMA	0.7053	0.006	0.807	0.9877	0.0024
	iPMMA	0.6353	0.026	0.846	0.9993	0.0026
	sPMMA	0.9309	0.051	0.577	0.9732	0.0019

R = correlation coefficient; S = standard error.

increase of temperature can be attributed to the entropy effect. However, when the temperature is elevated to 40°C, the equilibrium state can not be attained within 90 min, and the ESP estimated by extrapolation to the $t = \infty$ is 7.8 mN/m. The decrease of the ESP at 40°C indicates the importance of other factors, which may surpass the effect of entropy. When the pressure relaxation is initiated at a higher surface pressure (30 mN/m), it would be difficult to reach the equilibrium state since a vigorous nucleation and growth behavior should be involved. However, it is interesting to find that sPMMA exhibits an opposite behavior to that at π = 10 mN/m, becoming the least stable one among the three PMMA monolayers. It should be noted that, although the initial surface pressure are controlled in the relaxation experiment, the occupied areas corresponding to a PMMA molecule are different for the three stereoisomers. According to the isotherm shown in Figure 1, the area difference between iPMMA and sPMMA monolayers when compressed to 30 mN/m is about 4 Å²/repeat unit. The large area difference
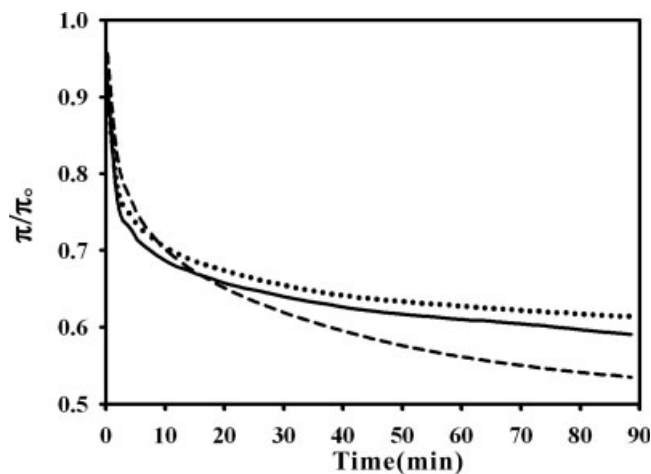

Figure 5 Pressure relaxation curves at 30 mN/m (40°C) [symbols as in Fig. 1(a)].

sure (ESP) of a monolayer by the pressure relaxation. According to the present results, the ESP of sPMMA can be estimated to be 8.5 mN/m at 10°C and 9.5 mN/m at 25°C. The increase of the ESP with the
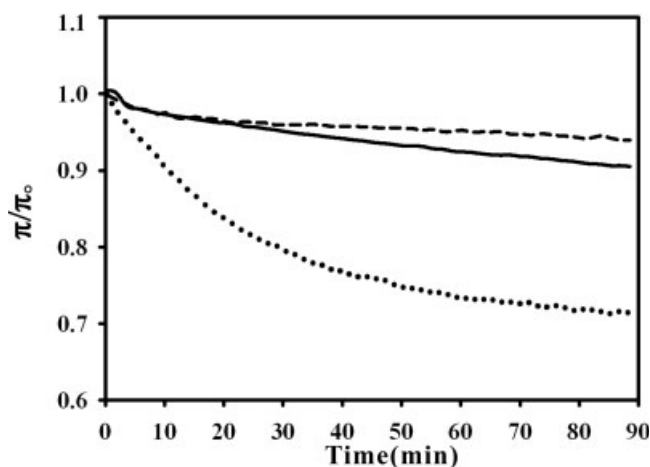
Figure 6 Pressure relaxation curves at 10 mN/m (40°C) [symbols as in Fig. 1(a)].

per repeat unit also indicates a great difference in the molecular density and the available area to perform the relaxation. In the present case, the higher pressure loss of sPMMA is probably caused by its higher available area, which gives more space for polymer chains orientation and relaxation.

For relaxation of a polymer monolayer, not only the nucleation and growth of 3D aggregates, but also the orientation transformation of the polymer chains should contribute to the pressure or area loss. The mechanism involved in the relaxation of a polymer monolayer is much more complicated than a monolayer of small molecule. This is also why more complicated results were observed in this work. The pressure relaxation results simulated by eq. (1) were tabulated in Table IV (at 30 mN/m) and Table V (at 10 mN/m). The agreement between data and simulation is reasonably good based on high correlation coefficient and small standard error deviation. The k_x and x values resemble those deduced from area relaxation.

TABLE IV
Modeling Parameters of Pressure Relaxation of PMMA at 30 mN/m at 10, 25, and 40°C

		π_∞/π_0	k_x	x	R	S
10°C	aPMMA	0.6104	0.426	0.426	0.9948	0.0053
	iPMMA	0.6831	0.349	0.385	0.9969	0.0003
	sPMMA	0.5526	0.215	0.544	0.9990	0.0035
25°C	aPMMA	0.6315	0.578	0.359	0.9919	0.0050
	iPMMA	0.6667	0.471	0.382	0.9954	0.0040
	sPMMA	0.5793	0.292	0.471	0.9989	0.0030
40°C	aPMMA	0.5751	0.577	0.359	0.9917	0.0061
	iPMMA	0.6090	0.563	0.406	0.9941	0.0050
	sPMMA	0.5101	0.299	0.488	0.9962	0.0066

R = correlation coefficient; S = standard error.

TABLE V
Modeling Parameters of Pressure Relaxation of PMMA at 10 mN/m at 10, 25, and 40°C

		π_∞/π_0	k_x	x	R	S
10°C	aPMMA	0.7453	0.020	0.585	0.9858	0.0025
	iPMMA	0.1779	0.027	0.519	0.9983	0.0028
	sPMMA	0.8482	0.386	0.616	0.9926	0.0009
25°C	aPMMA	0.5195	0.016	0.692	0.9941	0.0041
	iPMMA	0.7448	0.091	0.588	0.9988	0.0020
	sPMMA	0.9507	0.288	0.760	0.9926	0.0009
40°C	aPMMA	0.8194	0.025	0.752	0.9964	0.0021
	iPMMA	0.6243	0.063	0.723	0.9937	0.0085
	sPMMA	0.7769	0.046	0.420	0.9865	0.0021

R = correlation coefficient; S = standard error.

Temperature dependence of simulated k_x and x values

Since at 30 mN/m, iPMMA, aPMMA, and sPMMA are all above their highest inflection pressure, they are in the similar phase. Therefore, the k_x and x values of Table II at 30 mN/m for area relaxation were taken and plotted versus $1/T$ for comparison. The results were given in Figure 7. The x values were almost independent of both temperature and stereoregularity indicating very similar nucleation/growth mechanism. The rate constant (k_x) decreases as a result of temperature elevation. In the same way, the k_x and x values fixed at the area at a initial pressure of 30 mN/m were plotted in Figure 8 versus the inverse of temperature. The x values of aPMMA and sPMMA demonstrated slight increase as a result of temperature depression. For iPMMA, the x values are independent of temperature. The rate constant increases with increasing temperature regardless of tacticity. The order of the rate constants is as the following: aPMMA > iPMMA > sPMMA.
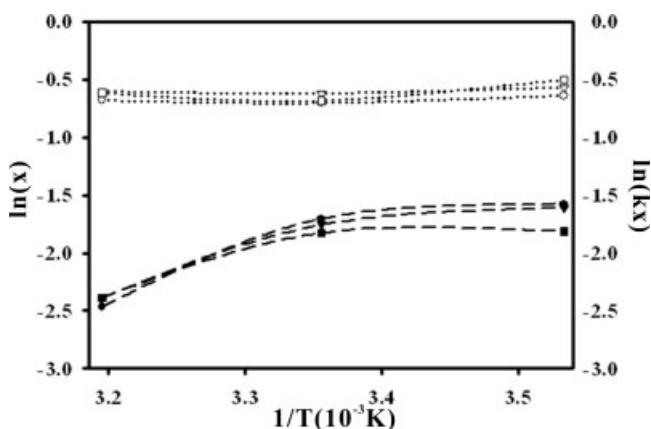

Figure 7 $\ln(k_x)$ and $\ln(x)$ versus $1/T$ (area relaxation). $\ln(k_x)$: ▼, iPMMA; ●, aPMMA; ■, sPMMA. $\ln(x)$: ▽, iPMMA; ○, aPMMA; □, sPMMA.
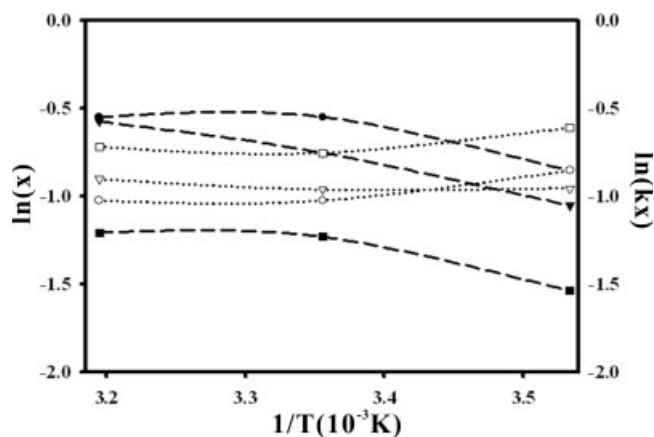
Figure 8 $\ln(k_x)$ and $\ln(x)$ versus $1/T$ (pressure relaxation) (symbols as in Fig. 7).

CONCLUSIONS

π-A isotherms of stereoregular PMMA were investigated at three different temperatures. The experimental results indicated that the collapse pressure and pressure at inflection point decrease with increasing temperature.

On the basis of simulation of area and pressure relaxation, similar nucleation/growth mechanism was responsible for the observed relaxation. For area relaxation at 30 mN/m, the computed k_x and x values were similar regardless of tacticity. The x values were found to be almost temperature-independent. However, the k_x values decreased as a result of temperature elevation. Although more complex mechanism was responsible for pressure relaxation, the simulated results were found to have a qualitative

resemblance to area relaxation. The x values were found to have minor temperature dependence. However, the k_x values were determined to increase with increasing temperature different from the findings of area relaxation.

References

1. Crisp, D. J. J Colloid Sci 1946, 1, 49.
2. Crisp, D. J. J Colloid Sci 1946, 1, 161.
3. Stroeve, P.; Srinivasan, M. P.; Higgins, B. G.; Kowel, S. T. Thin Solid Films 1987, 146, 209.
4. Baglioni, P.; Dei, L.; Puggelli, M. Colloid Polym Sci 1985, 283, 266.
5. Gabrielli, G.; Puggelli, M.; Faccioli, R. J Colloid Interface Sci 1972, 11, 63.
6. Gabrielli, G.; Puggelli, M.; Baglioni, P. J Colloid Interface Sci 1982, 86, 485.
7. Beredjick, N.; Ahlbeck, R. A.; Kwei, T. K.; Ries, H. E., Jr. J Polym Sci 1960, 46, 268.
8. Sutherland, J. E.; Miller, M. L. J Polym Sci Part B: Polym Lett 1969, 7, 871.
9. Brinkhuis, R. H. G.; Schouten, A. J. Macromolecules 1991, 24, 1487.
10. Brinkhuis, R. H. G.; Schouten, A. J. Macromolecules 1992, 25, 5692.
11. Brinkhuis, R. H. G.; Schouten, A. J. Macromolecules 1992, 25, 2725.
12. Hsu, W. P.; Lee, Y. L.; Liou, S. H. Appl Surf Sci 2006, 252, 4312.
13. Avrami, M. J Chem Phys 1939, 7, 1103.
14. Avrami, M. J Chem Phys 1940, 8, 212.
15. Avrami, M. J Chem Phys 1941, 9, 177.
16. Hsu, W. P.; Yeh, C. F. J Appl Polym Sci 1999, 73, 431.
17. Grohens, Y.; Hamon, L.; Reiter, G.; Soldera, A.; Holl, Y. Eur Phys J 2002, E8, 217.
18. Vollhardt, D.; Retter, U. J Phys Chem 1991, 95, 3723.
19. Vollhardt, D.; Retter, U. Thin Solid Films 1991, 199, 189.
20. Vollhardt, D.; Retter, U. Langmuir 1992, 14, 309.